

INVESTIGATION ON DISSOLUTION PROCESS OF THE STONES THROUGH THE ANALYSES OF CRYSTALLINE AND AMORPHOUS PHASES

ELISABETTA NEGRI

Dipartimento di Scienze della Terra, Università di Pavia, Via Ferrata 1, I-27100 Pavia

INTRODUCTION

The common hollow glass is often affected by “stones”: Al-rich crystalline inclusions representing the most widespread defects for the glass industry. Chiefly the stones derive from refractory materials of the furnace, contaminants introduced by raw materials and recycled cullet, incomplete melting of batch materials etc. (Falcone *et al.*, 2008a; Messiga *et al.*, 2008). Their presence is particularly dangerous because stones create high tension in glass, reducing the mechanical strength of the glass articles (Negri, 2007; Falcone *et al.*, 2008b). The chemical and physical features of these stones can vary significantly according to their origin, dwelling time in the glass melt, temperature, viscosity, etc. (Falcone *et al.*, 2008b). The stones are characterized by complex chemical compositions and microstructures as a consequence of transformation of the original material (Falcone *et al.*, 2008a). Re-crystallized and glassy phases usually surround the relicts of the pristine material (Falcone *et al.*, 2008a).

An understanding of the transformation mechanisms of such defects is fundamental in order to recognize the origin of the stones and to define suitable actions to eliminate or reduce them (Falcone *et al.*, 2008b).

The petrographic approach to the study of these defects is aimed to determine the reactions occurring between stones and molten glass, in order to understand the diffusion mechanisms responsible for the complete dissolution of the stone and to minimize this technological problem. For this purpose laboratory tests were performed in order to investigate the reaction sequence and to evaluate the influence exerted by Na⁺ and K⁺ ions on the dissolution process.

μ-Raman spectroscopy, SEM backscattered images, x-ray microanalysis and elemental maps were used to examine microstructural features and related composition of the samples. Moreover X-ray fluorescence spectrometry (XRF) and diffraction (XRD) were used to carry out bulk analyses on the materials used for the tests (ceramics and refractory).

Furthermore the reactions occurring between stone and glass were studied by applying the steady diffusion model of Joesten (Joesten, 1977; Negri, 2007; Messiga *et al.*, 2008). The reactions are dominated by the relative diffusion fluxes through the crystalline and glassy layers, involving Al³⁺, Na⁺ and K⁺ ions (Negri, 2007). The Joesten's modeling also stresses the role of alkaline elements, especially of potassium, in the dissolution process of the stones and it provides useful hints to control the development of reaction rim.

EXPERIMENTAL

In order to investigate the influence exerted by Na⁺ and K⁺ ions on the dissolution process of the Al-rich stones, some laboratory tests were carried out. For this purpose four alkalis-lime-silica glasses were prepared with constant molar content of alkaline oxides but with different Na₂O/K₂O ratios. A

sodium-lime glass (N), a potassium-lime glass (K), a mixed alkaline glass with Na₂O/K₂O ratio 1:1 (NK1) and mixed alkaline glass with Na₂O/K₂O 6:1 ratio (NK6) were prepared by melting the batches in an electric furnace at 1450°C. The chemical composition of each glasses is reported in Table 1. After melting, the glasses were quenched in water (frit) (Falcone *et al.*, 2008b).

Bars of a ceramic tableware (Al₂O₃ < 25 wt.%, see Table 1), representative of common ceramic findings in foreign glass cullet were used for the tests (Falcone *et al.*, 2008b). The ceramic bars were immersed in several Pt crucibles containing 600 g of the different frit glasses and subjected to the following thermal cycle: 32 hours at 1300°C followed by 12 hours at 1150°C (Negri, 2007; Falcone *et al.*, 2008b).

The same procedure was utilized with refractory bars (Al₂O₃ < 70 wt.%, see Table 1) usually employed into the furnace (Table 1) (Negri, 2007). A typical characteristic of a refractory is its lower porosity respect to the ceramic material and a better resistance to the corrosion process. For this reason the thermal cycle was necessary modified as follows: 72 hours at 1300°C and then 12 hours at 1150°C.

Table 1 – Chemical composition in wt.% of material used for the tests: C ceramic, R refractory, N sodium-lime silica glass, K potassium-lime silica glass, NK1 mixed alkaline glass with Na₂O/K₂O ratio 1:1 and NK6 a mixed alkaline glass with Na₂O/K₂O ratio 6:1 (Negri, 2007; Falcone *et al.*, 2008a; Messiga *et al.*, 2008; Falcone *et al.*, 2008b; Galinetto *et al.*, 2008).

Wt. %	SiO ₂	Al ₂ O ₃	Na ₂ O	K ₂ O	CaO	TiO ₂	Fe ₂ O ₃	Cr ₂ O ₃
N	71		15		14			
K	65			21	14			
NK1	67		8	11	14			
NK6	70		13	2	15			
R	29.5	68.0					0.80	0.018
C	72	23	4	1				

After the extraction, all bars were annealed at 550°C (Falcone *et al.*, 2008b) and then cut as cross-sections. The cross-sections were embedded in acrylic resin, ground, polished and coated with carbon for microanalytical investigation (Galinetto *et al.*, 2008). Afterwards the samples were labeled in a way that the first letter indicates the bar used for the tests (R for refractory and C for ceramic) while the second letter is referred to the glass.

All the samples were analyzed by SEM-EDX and x-ray analysis for elemental and micro-textural characterization (Galinetto *et al.*, 2008). The samples were investigated by means of a Jeol 5900 scanning electron microscopy (SEM) equipped with an Oxford Isis 300 EDX X-ray microanalyses (Falcone *et al.*, 2008b). The observations were performed in backscattered electron mode (BSE), particularly suitable for the identification of the phases with different average atomic weight (Falcone *et al.*, 2008b). Moreover X-ray fluorescence spectrometry (XRF) using a Philips PW2400 sequential X-ray spectrometer (Falcone *et al.*, 2008b) was employed to carry out bulk analyses on the materials used for the tests (ceramic,

refractory and glass). Compositional and textural features were investigated by SEM-EDX, furthermore μ -Raman spectroscopy was applied to distinguish the glassy and crystalline phases (Negri, 2007).

RESULTS

Microtexture investigation

The analysed samples are characterized by reaction rims with different composition and microtexture. The interaction between glass and the aluminous materials (refractory and ceramic used for the tests) develops microstructures generally organized in several concentric rims (Negri, 2007). In Fig. 1-4 examples of ceramic and refractory samples are reported (Negri, 2007). The microstructures are different in each sample and depend from the composition of glass with which they react (Negri, 2007). The ceramic bars reacting with sodium-lime glasses (N, NK6) only produce a glassy phase (Fig. 1) while using potassium glasses (K, NK1) a rim with leucite crystals (Rim1 in Fig. 2) is developed (Negri, 2007).

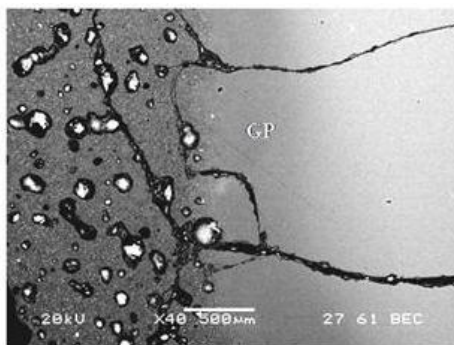


Fig. 1

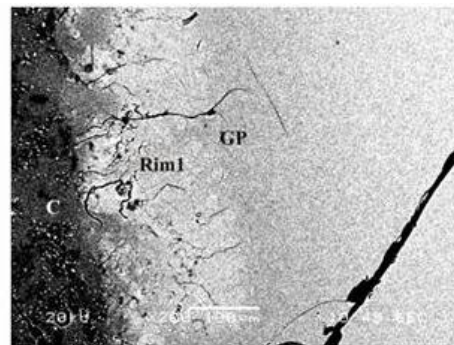


Fig. 2

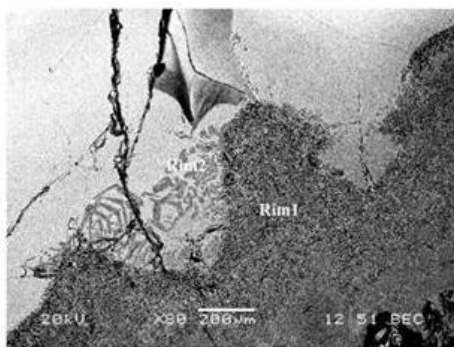


Fig. 3

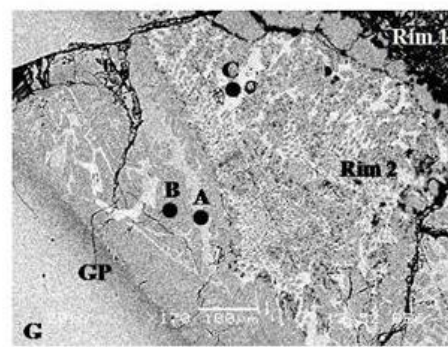


Fig. 4

Fig. 1 – SEM-BSE image of the C/NK6 sample at the ceramic/glass interface (C ceramic; GP glassy phase).

Fig. 2 – SEM-BSE image of the C/NK1 sample at the ceramic-glass interface. C ceramic; Rim1: sub-euhedral leucite crystals GP: glassy phase (Negri, 2007).

Fig. 3 – SEM-BSE image of the R/N sample at the refractory-glass interface. Rim1: nepheline matrix associated with needle-like corundum; Rim2: dendritic nepheline within the glassy ground mass (Negri, 2007).

Fig. 4 – SEM-BSE image of the R/NK1 sample; a detail of the refractory-glass interface. A, B, C, G μ -Raman investigated points; GP glassy phase (Falcone *et al.*, 2008a; Galinetto *et al.*, 2008).

The experimental results reveal for C/N and C/NK6 samples the total absence of secondary crystalline phases, while the microtextural features of the ceramic material are well preserved: needle-like

mullite crystals and sub-euhedral zircon crystals are well visible (Fig. 1,2). The ceramic/glass interface shows a homogeneous linear boundary (Fig. 1). The glassy phase (GP in Fig. 1), a compositional zoning within the glass with dark grey colour, is well developed (about 500 μm in size) and surrounds the ceramic.

On potassium glasses (K, NK1) and ceramic bars, secondary crystalline phases are observed. The C/K and C/NK1 samples are characterized by several concentric rims arrangement (Fig. 2). The ceramic microtexture is well preserved and it is surrounded by a rim (Rim1 in Fig. 2) made by sub-euhedral leucite crystals. A glassy phase (about 300 μm in size) enclosed the previous rim (GP in Fig. 2).

The refractory samples present the most complex microtextures (Negri, 2007). Moving from the refractory core to the glass, it is possible to observe a recurrent layer sequence: a rim (Rim1 in Fig. 3,4) with corundum crystals strictly in contact with the refractory, followed by a second rim (Rim2 in Fig 3,4) with feldspathoids and a glassy phase encloses all the previous rims (Negri, 2007).

The R/N sample (Fig. 3) obtained from the reaction between sodium-lime glass and refractory is characterized by considerable microtextural complexities. Moving from the refractory core to the glass a wide rim (600/800 μm in size) is observed (Rim1 in Fig. 3) with needle-like corundum crystals. The corundum crystals create a felt texture and sometimes the needle-like crystals are grouped in fascicular bundle. A second rim, surrounding the previous Rim1, is characterized by the presence of well developed nepheline dendrite (Fig. 3). A wide glassy phase enclosed all the previous concentric reaction layers. The R/NK6 sample in sodium glass shows the same microtextural arrangement of the R/N sample, nevertheless the nepheline shows a particular texture defined as “comb shaped” in which the nepheline is nucleated in roundish crystals lengthened parallel each other.

The reactions developed between potassium glass and refractory produce concentric reaction rims. In the R/K sample, strictly in contact with the refractory, a corundum rim is found again. From the corundum rim a very thin (< 5 μm in size) dendritic leucite microtexture is nucleated with only primary arms. A wide (about 400 μm in size) glassy phase is also present.

The R/NK1 sample presents the most complex microtexture, consisting of three rims (Fig. 4). Starting from the refractory moving to the glass a first rim (Rim1 in Fig. 4) consists of crystalline aggregates mainly containing corundum-needle like crystals (Falcone *et al.*, 2008a). The second rim (Rim2 in Fig. 4) is characterized by a sub-euhedral phase with feldspathoid-like composition; finally the outer rim is constituted by a modified glass layer (glassy phase, GP in Fig. 4) (Falcone *et al.*, 2008a). In detail, the first rim near the pristine material (Rim1 in Fig. 4) is characterized by an aggregate of needle-like corundum crystallizations (Falcone *et al.*, 2008a; Galinetto *et al.*, 2008). Rim2 displays a particularly complex microstructure consisting of a light grey phase with sharply shape (A in Fig. 4), a roundish grey phase (B in Fig. 4) and an interstitial white phase (C in Fig. 4) (Falcone *et al.*, 2008a). A glassy phase (GP in Fig. 4) surrounds Rim2 towards the glass (Falcone *et al.*, 2008a; Galinetto *et al.*, 2008). In this sample SEM/EDX analysis shows a “leucite-like” composition of phase B and two similar (but not identical) silica-alumina- soda-potash-lime compositions for the phases A and C (Falcone *et al.*, 2008a). The chemical compositions of the “leucite-like” and “nepheline-like” phases match the leucite and nepheline compositions reported in literature, but their roundish structure doesn't allow to distinguish between glassy and crystalline phases (Falcone *et al.*, 2008a). In order to investigate their structure, μ -Raman spectroscopy analysis was applied to the study of the R/NK1 sample (Falcone *et al.*, 2008a). The results are reported in Fig. 5. The spectrum G is collected from the glass and no relevant features are evidenced, as expected (Falcone *et al.*, 2008a). The spectrum collected at the point B is reported together with the

spectrum of a standard leucite mineral (Falcone *et al.*, 2008a). The good matching of the two spectra is evident (Falcone *et al.*, 2008a). In the spectra A and C a strong luminescence signal giving a shoulder which increases moving to higher energies is observed (Falcone *et al.*, 2008a). Similar signals are commonly referred to the presence of luminescent ions inside the analysed phases (Falcone *et al.*, 2008a). In this case this is probably due to the presence of Cr^{3+} ions, coming from the refractory (Falcone *et al.*, 2008a). A Cr_2O_3 amount of 0.018 wt.% was determined by XRF analysis in the Al-rich refractory (Table 1) (Falcone *et al.*, 2008a). The Cr^{3+} ion (even in traces) generates a strong luminescence signal whose shape depends on the structure of the host lattice (Falcone *et al.*, 2008a; Grinberg *et al.*, 2002). In spectrum C a strong luminescent emission and no structured Raman features are observed (Falcone *et al.*, 2008a). The absence of well defined Raman modes suggests that in this region there is a prevalence of a glassy phase (Falcone *et al.*, 2008a). In spectrum A the presence of intense luminescence does not hinder the detection of Raman structures in the region between 300 and 600 cm^{-1} indicating a partial crystallization in this area (Falcone *et al.*, 2008a). The Raman modes observed at around 500 cm^{-1} can be reasonably ascribed to the formation of leucite, while the weakness of the signals around 300-400 cm^{-1} (not ascribable to a leucite structure) (Falcone *et al.*, 2008a) is linked to calcsilite and indicate a partial crystallinity of the white phase.

Modelling

The presence of reaction rims is indicative of incomplete reactions in a non equilibrium system. This system is constrained by diffusion processes and the formation of the layers indicates an incomplete reaction due to differences in fluxes of the components within the reaction zone (Messiga *et al.*, 2008). Consequently the described layer sequences can be modellized using a steady state system, where the concentration gradients of the component migrating during the reactions are constant in time and space (Negri, 2007; Messiga *et al.*, 2008). This steady state is achieved by the system when the intake and the outtake rates of each component through a layer are controlled by diffusion (Negri, 2007; Messiga *et al.*, 2008). Therefore the reactions occurring at the stone/glass interfaces and producing the microtextures were modellized using the local equilibrium-steady diffusion model proposed by Fisher (1975) and Joesten (Joesten, 1977; Negri, 2007; Messiga *et al.*, 2008; Fisher, 1975). Joesten, following a first approach by Fischer, proposed a method for the calculation of the diffusion coefficients of the chemical elements during a reaction (Negri, 2007; Messiga *et al.*, 2008).

The first step of this model implies to calculate the empirical formula for each phase of the investigated system. The empirical formulas were calculated from the chemical composition (wt.% of the oxides) of each phase (Messiga *et al.*, 2008). The moles of each element were calculated and then divided by the lower molar value (Messiga *et al.*, 2008). The obtained values are the stoichiometry coefficients of the empirical formula; in this way all the stoichiometry coefficients have values equal or higher than 1 (Messiga *et al.*, 2008). As CaO resulted to be the less mobile oxide in the reaction band, in order to simplify the system only SiO_2 , K_2O and Al_2O_3 were considered and the compositions were then

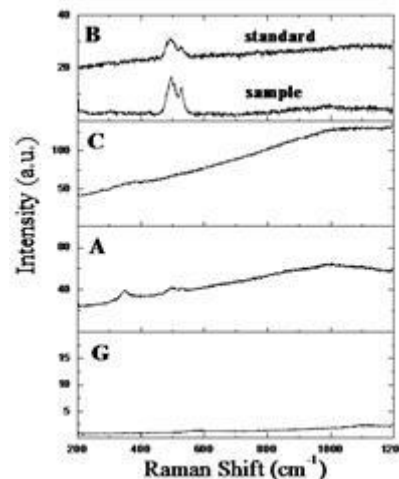


Fig. 5 – μ -Raman spectra of phases A, B, C, and G (Fig. 4) (Falcone *et al.*, 2008a).

normalized (Messiga *et al.*, 2008). Consequently, the system is characterized by 4 components and a reaction band composed by two phases (leucite or nepheline and glassy phase) (Messiga *et al.*, 2008).

In this model, the stoichiometry coefficients of the layer growth reactions were then computed from the mass balance at each layer/layer contact and from independent ratios of instantaneous fluxes within each layer (Negri, 2007; Messiga *et al.*, 2008). This modelling implies the setting of one mass balance equation and one steady diffusion equation for each of the diffusing components at each layer/layer contact and one flux ratio equation for each phase concerned (Negri, 2007). Solving the linear equations system by a matrix inversion computer program, all the possible permutations of the diffusion values for Al, Na, K and Si can be calculated (Negri, 2007).

The model shows a wide diffusion range of Sodium and a scanty mobility for aluminium when ceramic reacts with sodium glasses (C/N, C/NK6) (Negri, 2007). Consequently the nucleation of feldspathoid crystals is hindered by a scanty mobility of aluminium and by the presence of limited catalytic factors as sodium and silica. Aluminium diffuses slowly also in ceramic samples with potassium glasses (C/K, C/NK1); so the formation of the secondary crystalline phases is mainly due to the high diffusion velocity of potassium than aluminium.

The behavior of aluminium is different in the refractory samples (Negri, 2007). By the way, high mobility for aluminium and a wide diffusion range for Na, K and Silica characterized the R/N and R/NK6 samples. The high mobility of the chemical elements in the R/N and R/NK6 samples are also responsible for the formation of quite developed nepheline crystals. Finally, the leucite crystals formed in refractory samples reacted with potassium glass (R/K, R/NK1) are due to a reduction of diffusion velocity of potassium in favour of aluminium (Negri, 2007). The R/NK1 sample shows the widest reaction rim in which potash secondary crystalline phases as leucite and calsilite prevailing. The total absence of Sodium-rich phases like nepheline for example, is due to diffusion process controlled by aluminium. Low diffusion rate of aluminium and contemporary high diffusion rate of alkaline elements are responsible of the observed reaction rims and the destabilization of leucite crystals.

CONCLUSION

In this work Al-rich stones obtained from laboratory tests were analysed in order to understand the dissolution process responsible for the complete dissolution of this technological problem.

The samples were obtained from laboratory tests in which different kind of aluminous material (ceramic and refractory) and appropriate glasses were used. Microstructural analyses and diffusion modelling were then carried out on the laboratory samples. The different glasses employed during the tests are responsible for the different microtexture arrangements characterizing the samples.

In the ceramic samples, secondary crystalline phases were founded only in potassium glasses while wide glassy phases were detected in the ceramic samples with sodium glass. In the ceramic samples is well evident an opposite behaviour of the alkaline elements: Sodium characterizes the glassy phase while Potassium the secondary crystalline phases.

In the refractory samples the opposite behaviour for the alkaline elements is also emphasized.

The nucleation of secondary crystalline phases is above all influenced by the Potassium while Sodium promotes the formation of glassy phase. This is particularly emphasized in the RNK1 sample, in which sodium secondary crystalline phases (nepheline) were not recognized. Anyway, secondary crystalline phases (feldspathoids) were formed in all refractory samples.

The Joesten's model stresses the different behavior of the alkaline elements mostly related to the different amount of aluminium involved in the reactions. The model evidences that in ceramic samples the formation of glassy phase is promoted if the diffusion velocity of alkaline elements, in particular of Sodium, is lower than aluminium. The nucleation of secondary crystalline phases is due to a high diffusion of potassium than sodium and aluminium. An opposite trend is observed in the refractory samples, where the microtextures are mainly due to the high mobility of aluminium rather than alkaline elements (Negri, 2007).

The Joesten's model provides helpful data which can be used to destabilize or hinder the formation of a reaction rim. The microtexture and microanalytical investigations associated to the modelling proved to be a successful approach to the comprehension of such defect which can be suggested to the hollow glass industry for the treatment and the resolution of this technological problem.

ACKNOWLEDGMENTS

The experimental part of this research was carried out by the Stazione Sperimentale del Vetro, Murano (VE).

REFERENCES

- Falcone, R., Galinetto, P., Messiga, B., Negri, E., Riccardi, M.P., Sommariva, G., Verità, M. (2008a): Combined SEM-EDX and μ -Raman spectroscopy for the characterisation of glass/refractory interfaces. *Microchimica Acta*, in press.
- Falcone, R., Messiga, B., Negri, E., Profilo, B., Riccardi, M.P., Sommariva, G., Verità, M. (2008b): Al_2O_3 - SiO_2 stones in glass: a study of dissolution processes. *Glass Technol.*, in press.
- Fisher, G.W. (1975): The thermodynamics of diffusion controlled metamorphic processes. In "Mass transport phenomena in ceramics", A.R. Cooper & A.H. Heuer, eds. Plenum, New York, 111-122.
- Galinetto, P., Falcone, R., Negri, E., Verità, M. (2008): μ -Raman spectroscopy characterisation of glass/refractory interfaces: a tool to improve the quality of the industrial glass production. *J. Raman Spectrosc.*, in press.
- Grinberg, M., Barzowska, J., Shen, Y.R., Bray, K.L., Padlyak, B.V., Buchynskii, P.P. (2002): High-pressure luminescence of Cr^{3+} doped $\text{CaO-Ga}_2\text{O}_3\text{-GeO}_2$ glasses. *Phys. Rev. B*, **65**, 064203/1-9.
- Joesten, R. (1977): Evolution of mineral assemblage zoning in diffusion metasomatism. *Geochim. Cosmochim. Acta*, **41**, 649-670.
- Messiga, B., Negri, E., Riccardi, M.P., Falcone, R., Profilo, B., Sommariva, G., Verità, M. (2008): Study and modellization of Al_2O_3 - SiO_2 stones dissolution in alkalis-lime silica melts. *Glass Technol.*, submitted.
- Negri, E. (2007): The stones into the hollow glass: investigation on dissolution process. *Scient. Acta*, **1**, 39-42.